

Mössbauer-effect investigation of a Cr—13.5 at. % Fe alloy doped with 0.7 at. % ^{119}Sn

S. M. Dubiel,* Ch. Sauer, and W. Zinn

Institut für Festkörperforschung der Kernforschungsanlage, Postfach 1913 D-5170 Jülich, West Germany

(Received 26 April 1985)

Cr—13.5 at. % Fe alloy doped with 0.7 at. % ^{119}Sn is studied at temperatures T from 4.2 to 330 K using Mössbauer-effect spectroscopy at ^{57}Fe and ^{119}Sn sites. The temperature dependence of the hyperfine (hf) fields H and isomer shifts I indicates that the alloy undergoes a reentrant transition on lowering T , from a paramagnetic (PM) through an antiferromagnetic (AFM) to a spin-glass (SG) state, in agreement with a recently published phase diagram [S. K. Burke *et al.*, *J. Phys. F* **13**, 451 (1983)]. Both magnetic states are found to be heterogeneous, containing a PM phase in addition. The PM part varies with T and amounts to $\sim 75\%$ in the AFM phase just above the transition temperature (AFM \rightarrow SG) and drops to $\sim 25\%$ when entering the SG phase ($T \simeq 20$ K). Comparison with recently obtained results for an Fe—25 at. % Cr alloy [S. M. Dubiel, Ch. Sauer, and W. Zinn, *Phys. Rev. B* **30**, 6285 (1984)] is made and discussed.

I. INTRODUCTION

Although $\text{Cr}_{1-x}\text{Fe}_x$ alloys have been the subject of numerous investigations, the understanding of their magnetic properties is still far from being clear and satisfactory, especially for $x < 0.30$. In this region, the phase diagram of the system seems to be rather complex,¹ and its boundaries have not yet been completely worked out.

Often, different experimental techniques used to study the magnetic properties of the system yield results which do not agree well with each other. It seems, however, that the main reason for the discrepancies lies not in the experimental methods, but rather in the samples themselves. There is a lot of evidence that their magnetic properties depend very sensitively on the actual distribution of the Fe atoms in the Cr matrix. In other words, samples having the same nominal composition exhibit different magnetic characteristics depending on their chemical homogeneity. It seems therefore useful to apply first of all microscopic methods in order to understand the relationship between the magnetic properties of the alloy and its microstructure. In our recent study on an Cr—25 at. % Fe alloy, we applied for this purpose Mössbauer-effect spectroscopy² and we showed, among other things, that although the alloy is chemically homogeneous, it is magnetically very heterogeneous: The transition from the paramagnetic to the ferromagnetic phase is not well defined, because the latter phase consists of several sub-phases becoming magnetic at different T . On further lowering of T this magnetic phase transforms into another magnetic state which we have identified by our recent in-field Mössbauer-effect measurements³ as a spin-glass state.

It is interesting to see the results obtained with the same method for an alloy composition which, according to a recently published phase diagram, should undergo a reentrant phase transition from a paramagnetic through an antiferromagnetic to a spin-glass state. For that purpose we have chosen a Cr—13.5 at. % Fe alloy as the subject of our present investigation.

II. EXPERIMENTAL

A. Sample preparation

We melted 330 mg of the $\text{Cr}_{867}\text{Fe}_{133}$ master alloy (nominal composition), which was kindly supplied by Burke together with 7.6 mg of tin enriched to $\approx 91\%$ ^{119}Sn in an arc furnace under a pure argon atmosphere. The ingot obtained was next remelted in an induction furnace under an argon atmosphere. Finally, the sample was annealed at $T = 1000^\circ\text{C}$ for 24 h and oil-quenched afterward.

This treatment resulted in a total mass loss of 6.5 mg. It should be noted that a $\text{Cr}_{75}\text{Fe}_{25}$ alloy subjected to a similar homogenizing treatment² turned out to be chemically homogeneous within $\pm 10\%$. The chemical analysis carried out on a part of the final sample gave the following composition: 13.5 at. % Fe, 85.8 at. % Cr, and 0.7 at. % Sn.

B. Mössbauer-effect measurements

For the Mössbauer-effect (ME) measurements the sample was filed to a powder with an average particle size of $\sim 60 \mu\text{m}$. It was placed in a helium flow cryostat which stabilized the temperature within 0.1–1 K, depending on the temperature range.

The measurements were carried out by means of a standard spectrometer with a sinusoidal drive and a 512-channel analyzer. The spectra were registered both at ^{57}Fe and ^{119}Sn nuclei. For the ^{57}Fe the 14.4-keV γ rays were supplied by a ^{57}Co source in rhodium, and for ^{119}Sn a $\text{Ca } ^{119}\text{SnO}_3$ source was used as an emitter of the 23.8-keV γ rays. Spectra of high statistical quality could be collected within 24–36 h for ^{57}Fe and 48 h for ^{119}Sn , respectively. The calibration procedure was carried out using an Fe metallic foil and BaSnO_3 powder as standards.

III. RESULTS AND THEIR DISCUSSION

A. ^{57}Fe -site results

Figure 1 shows some examples of the ^{57}Fe -site Mössbauer spectra at different temperatures T . The spectra reveal the following features: (i) They are not well-resolved even at low T and (ii) they are symmetric. The latter feature justifies the application of the hf field distribution fitting method for their analysis as outlined by Window.⁴

This method is model independent and yields the hf field distributions. Those distributions corresponding to the spectra shown in Fig. 1 are presented in Fig. 2. As can be seen they reflect in an instructive way the influence of T on the magnetic state of the studied sample. In particular, we can note that the transition from a paramag-

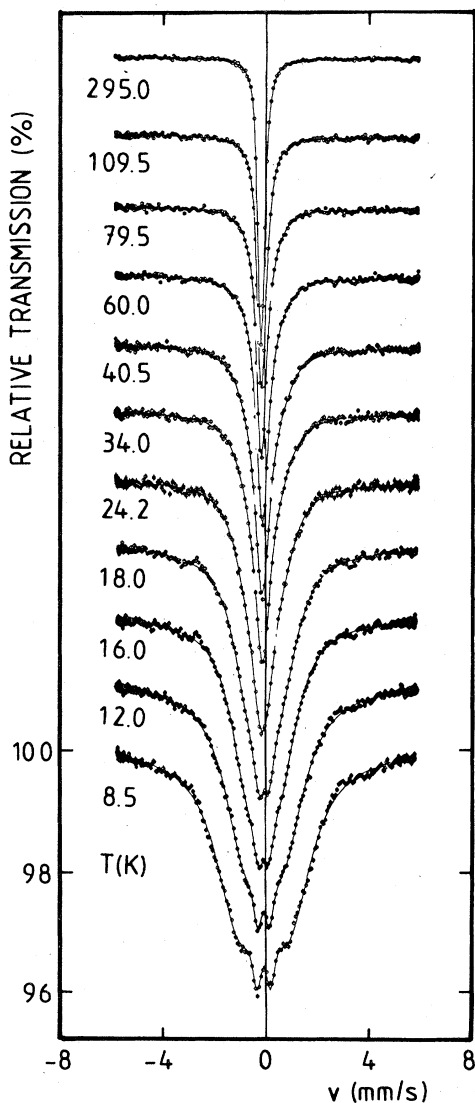


FIG. 1. ^{57}Fe -site Mössbauer spectra of the Cr-13.5 at. % Fe alloy at different temperatures. The solid lines represent the fit using the Window's method (see text).

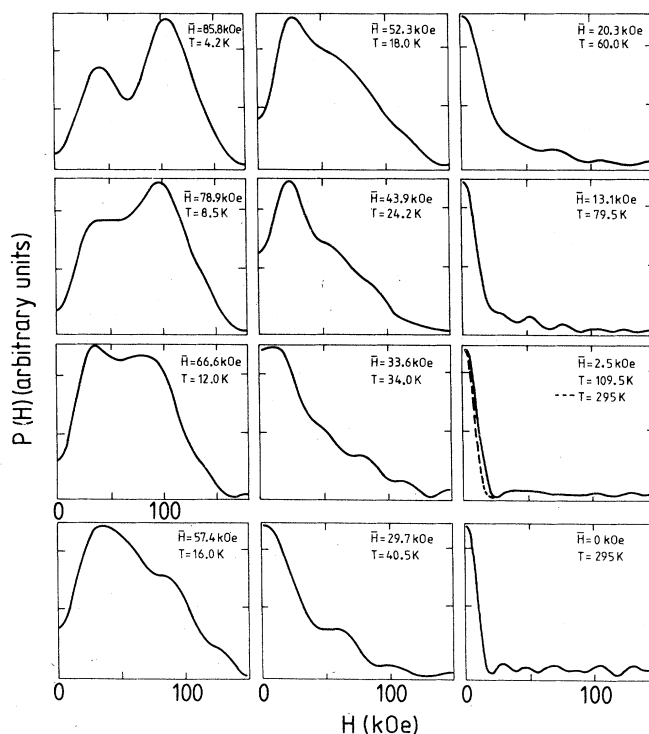


FIG. 2. Hyperfine field distributions as obtained from the spectra shown in Fig. 1 by Window's method (Ref. 4). \bar{H} gives the average value of the hf field.

netic (PM) to an antiferromagnetic (AFM) phase is not sharp, i.e., the sample as a whole does not become magnetic at one well-defined temperature. According to Burke and Rainford⁵ the Néel temperature for this composition amounts to $T_N \approx 90$ K, i.e., at 79.5 K our sample should be already in the AFM state, and consequently the corresponding hf field distribution should be homogeneously broadened in comparison with its shape at $T > T_N$. Instead, in addition to a dominating single-peak distribution at $H=0$, there are additional peaks at higher H indicating the presence of a magnetic phase in the sample. Further decrease of T broadens slowly the single-peak contribution. Simultaneously one observes the development of the higher field components whose contributions become more important with decreasing T .

The hf field distributions prove, therefore, that comparable to the Cr-25 at. % Fe alloy,² in this sample also the coexistence of a low-field and a high-field component can be observed, the latter one exhibiting some additional structure. Such a distribution indicates a heterogeneous character for the antiferromagnetic phase of the sample studied. Here, however, the heterogeneity is not so well pronounced compared with the Cr-25 at. % Fe sample. This may be due to the spin-density waves (SDW), which have itinerant character and can weaken the deviations between different antiferromagnetic environments present in the sample. On the other hand, the SDW should be less intensive in the sample with higher iron concentration, and consequently the heterogeneous character of its magnetism should be more pronounced. In addition, as

we shall see below, the present sample is chemically less homogeneous than the Cr-25 at. % Fe one. The Fe atoms are partly clustered, and this obviously smears out the differences between different atomic configurations.

It should be also mentioned that the broadening of the single peak in the hf field distribution can be observed at $T = 109.5$ K, i.e., at $T > T_N$. It is, however, "normal" in that, due to the time-scale involved in the ME experiments, this technique can reveal such spin-density correlations above T_C or T_N .

From the hf field distributions we evaluate the average hf fields, \bar{H} by integrating the $P(H)$ curves over H . The values obtained on that way are given in Fig. 2, and plotted against T in Fig. 3 as full circles. The corresponding behavior obtained previously for the alloy containing 25 at. % Fe has been marked by the dashed line for comparison. Concerning the present data, we note that \bar{H} remains zero down to $T \sim 150$ K where it starts slowly to increase on lowering T . At $T \sim 80$ K the rate of increase becomes larger and stays rather constant until T drops to 25 K. Below this temperature, \bar{H} increases still faster with the maximum rate at $T = 10$ K [see inset (a) in Fig. 3]. This behavior, as a whole, resembles that found for the Cr-25 at. % Fe alloy.² The main difference occurs at the tail which is more extended for the less concentrated sample, i.e., the Néel temperature for this sample is less

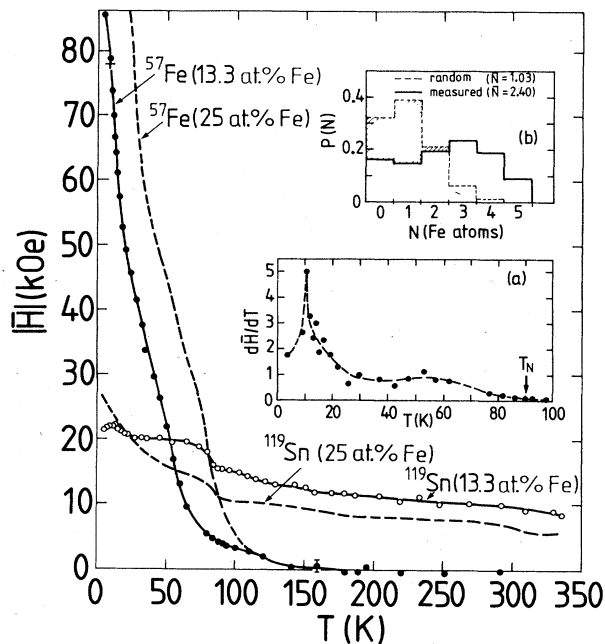


FIG. 3. Average hf field \bar{H} vs temperature T . The open circles show \bar{H} at the ^{119}Sn site, and the closed circles at the ^{57}Fe site, respectively (+ indicates the value of \bar{H} obtained with the superposition method). The dashed lines indicate the corresponding fields as obtained for the Cr-25 at. % Fe sample investigated in Ref. 2. The temperature derivative of the ^{57}Fe site \bar{H} is shown as inset (a) with T_N marking the Néel temperature after Ref. 5. Inset (b) shows the probability $P(N)$ for finding N Fe atoms in the nearest-neighbor shell around an ^{57}Fe probe atom as measured (—) and as expected for a random Fe-Cr distribution (---), respectively.

well defined than the Curie temperature for the more concentrated sample (this, in our opinion reflects the chemical heterogeneity of the present sample). Furthermore, \bar{H} (13.5 at. % Fe) is shifted by ~ 25 K toward lower T with respect to \bar{H} (25 at. % Fe).

Concerning the spin-freezing temperature T_f it is still better defined through the $d\bar{H}/dT$ -versus- T curve [see the inset (a) in Fig. 3]. We see, therefore, that the process of the spin freezing starts at $T_f \simeq 25$ K, while the majority of "objects" freeze at $T_f \simeq 10$ K. The latter value agrees very well with $T_f = 9$ K deduced by the authors of Ref. 5 for the same composition.

As we mentioned above, the shapes of the hf field distributions shown in Fig. 2 are justified regarding the sample as consisting of a magnetic (M) and a nonmagnetic (NM) phase. A similar feature was revealed for the Cr-25 at. % Fe sample that Hesse *et al.*⁶ presented for the $\text{Cr}_{1-x}\text{Fe}_x$ alloys, $0.24 \leq x \leq 0.31$, where the amount of the M phase, A_M , depends for a given composition substantially on the heat treatment, i.e., on the actual distribution of atoms. In other words, A_M is indicative of the chemical heterogeneity of a sample.

In order to see whether the present sample is chemically homogeneous, we fitted the spectra assuming they consist of two parts: a single-line part corresponding to the NM phase and a six-line part related to the M phase. The abundance of the M phase, A_M was calculated from the following formula:

$$A_M(\%) = 100S_M/S_T, \quad (1)$$

where S_M is the area of the magnetic subspectrum and S_T is the area of the total spectrum. Figure 4 illustrates the A_M values versus T . For comparison, the corresponding behavior found previously for the Cr-25 at. % Fe sample² is included, as well.

We see that the behavior of A_M (13.5 at. % Fe) differs distinctly from that of A_M (25 at. % Fe). In particular, a steplike change observed for the higher Fe concentration cannot be seen now. Instead, two regions can be distinguished by a characteristic temperature $T(A_M) \simeq 21$ K. Above this temperature, i.e., within the AFM regime, A_M

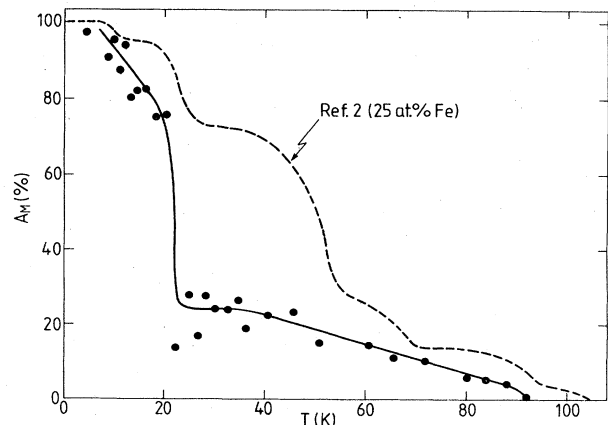


FIG. 4. Abundance of the magnetic phase A_M vs temperature T . The dashed line indicates A_M as measured for the Cr-25 at. % Fe sample (Ref. 2).

increases slowly with decreasing T ; below $T(A_M)$, i.e., within the spin-glass (SG) regime, A_M develops quickly on lowering T . This suggests that one has to distinguish between the mechanism responsible for the quenching of the NM phase in the AMF regime ($T \geq 21$ K) and the one in the SG regime ($T \leq 21$ K). The latter obviously is much more efficient.

The distinction between the M and NM phases seems also to be supported by the isomer shifts I related to the two phases. As illustrated in Fig. 5, which shows I_M and I_{NM} versus T , $|I_{NM}| > |I_M|$ for all T . As both I_M and I_{NM} are negative, this means that the charge density at Fe nuclei in the M phase is smaller compared with the charge density in the NM phase. It is known (see, e.g., Refs. 7 and 8) that the isomer shift becomes more negative with decreasing Fe concentration, i.e., with decreasing number of Fe neighbors. The present finding agrees with this tendency. Therefore, it is justified to relate I_{NM} with the Fe nuclei having less Fe neighbors, hence being nonmagnetic, and I_M with those Fe nuclei having an iron-rich surrounding, hence being magnetic. We shall see below that a similar behavior of I is obtained applying a still more exact superposition method for fitting the spectra.

We can even go one step further and estimate the average number of the Fe atoms in the first-neighbor shell \bar{N} for the two kinds of environments. For that purpose we use a relationship between the Fe-site average isomer shift, \bar{I} and the concentration of iron, x in $\text{Cr}_{1-x}\text{Fe}_x$ alloys given in Ref. 7:

$$\bar{I} = -0.145x \quad (2)$$

Using this relation together with our results $I_{NM} \simeq -0.120$ mm/s and $I_M \simeq -0.080$ mm/s, we obtain $x_{NM} \simeq 17$ at. % for the concentration of iron in the NM phase and $x_M \simeq 45$ at. % for the M phase (note that in both phases the iron content is larger than the bulk average; this may be understood in terms of clustering). Neglecting such a possible clustering and assuming that the distribution of Fe atoms within both phases is random, we can relate the iron concentration with the average number \bar{N} of Fe atoms in the first shell: $8x = \bar{N}$. This finally yields $\bar{N}_{NM} \simeq 1.4$ for the NM phase and $\bar{N}_M \simeq 3.6$ for the M phase. These figures seem to be

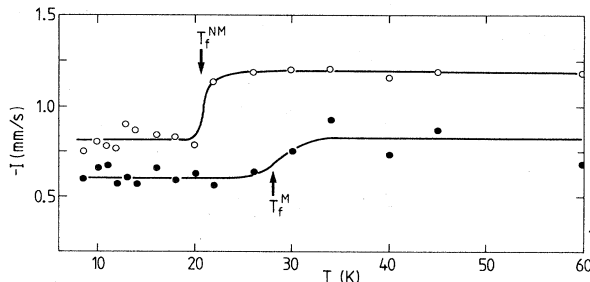


FIG. 5. Isomer shift of the nonmagnetic (NM) phase (open circles), and of the magnetic (M) phase (closed circles) vs temperature T . Note the different temperatures, where in both phases a step occurs, $\Delta T_f = T_f^{NM} - T_f^M \neq 0$.

reasonable and would mean that the Fe nuclei within the former phase have mainly none, one or two Fe neighbors, while those within the latter phase have mostly two, three, or four Fe neighbors [see also the inset (b) in Fig. 3].

It should also be noted that on lowering T , both I_{NM} and I_M show an anomaly. I_{NM} reveals a sharp step at $T_f^{NM} \simeq 21$ K, which coincides perfectly with the temperature at which A_M exhibits a sharp change, whereas I_M shows a less distinct discontinuity at $T_f^M \simeq 28$ K. The difference between T_f^{NM} and T_f^M is probably related to the difference in the Fe concentration in the two phases. This would agree, at least qualitatively, with the observation by Burke and Rainfold,⁵ that T_f increases with x . We observed recently a similar behavior for the Cr-25 at. % Fe sample, using in-field Mössbauer-effect measurements.³

Finally, we can check the chemical homogeneity of the studied sample by fitting the spectra using a superposition method. Here one assumes that each spectrum consists of several subspectra having different hf fields, $H(N)$, isomer shifts, $I(N)$, and probabilities, $P(N)$, with $N=0,1,\dots,5$ being the number of Fe atoms in the first-neighbor shell, NN. The best-fit parameters obtained in this way for the 8.5-K spectrum are presented in Table I. The values of the probabilities expected for the random distribution P_0 are also included. We see that the "measured" distribution differs from the expected one. In particular, the measured average number of Fe atoms in NN amounts to $\bar{N}=2.40$, while that one expected for a random distribution is $\bar{N}_0=1.03$. This shows in a quantitative way that the Fe atoms are clustered.

The values of the hf field $H(N)$ are also instructive. They permit us to determine the contribution ΔH to H by subsequent Fe atoms added to the first shell. The calculated values $\Delta H = H(N+1) - H(N)$ are included in Table I. It is worth noting that the ΔH values are fairly constant with an average of $\overline{\Delta H_e} = 25.2 \pm 0.1$ kOe for the even number of Fe neighbors and with $\overline{\Delta H_o} = 21.7 \pm 1.0$ kOe for the odd number of Fe neighbors. These data of ΔH prove that the contribution of the Fe atoms to the hf field is to a high-degree additive for this composition. It is interesting to compare the present result of ΔH with the corresponding one obtained for the Fe-rich $\text{Cr}_{1-x}\text{Fe}_x$ alloys,⁸ $\Delta H_1 = 31$ kOe. From the two figures we can conclude that ΔH has decreased by $\sim 23\%$ on lowering x to ~ 13 at. %. This decrease is only by $\sim 5\%$ larger than the corresponding decrease of the Fe-site magnetic moment ($\mu_{\text{Fe}} = 1.8\mu_B$ for $x \simeq 13$ at. %, after Ref. 9).

TABLE I. Best-fit values of the Fe-site hf field H (in kOe), isomer shift I (in mm/s), and configuration probabilities P of the 8.5-K spectrum. P_0 stands for the random distribution, N is the number of Fe atoms in the nearest-neighbor shell, and $\Delta H = H(N+1) - H(N)$.

N	H	ΔH	I	P	P_0
0	-21.2		-0.082	0.16	0.32
1	-46.3	25.1	-0.076	0.14	0.39
2	-67.4	21.1	-0.062	0.19	0.21
3	-92.6	25.2	-0.056	0.23	0.06
4	-115.5	22.9	-0.050	0.19	0.01
5	-140.7	25.2	-0.041	0.09	

B. ^{119}Sn -site results

Figure 6 illustrates several selected ^{119}Sn -site Mössbauer-spectra for different temperatures. In contrast to the ^{57}Fe -site spectra, they are asymmetric. Consequently, one cannot fit them with the simple hf field distribution method.⁴ Instead, we fitted them using the superposition method obtaining the hf fields $H(N)$, isomer shift $I(N)$, and the probabilities $P(N)$, of each contributing subspectrum. It turned out that we could consistently fit all the spectra with six subspectra ($N=0-5$). In Table II we have compiled the best-fit values of the hf parameters we obtained for the spectrum registered at 5.3 K.

Based on the $H(N)$ and $P(N)$ results, we evaluated the average hf field $\bar{H}_{\text{Sn}} = \sum_{N=0}^5 H(N)P(N)$ and plotted it in Fig. 3 (open circles). One readily can see that \bar{H}_{Sn} shows a quite different behavior versus T compared with that of

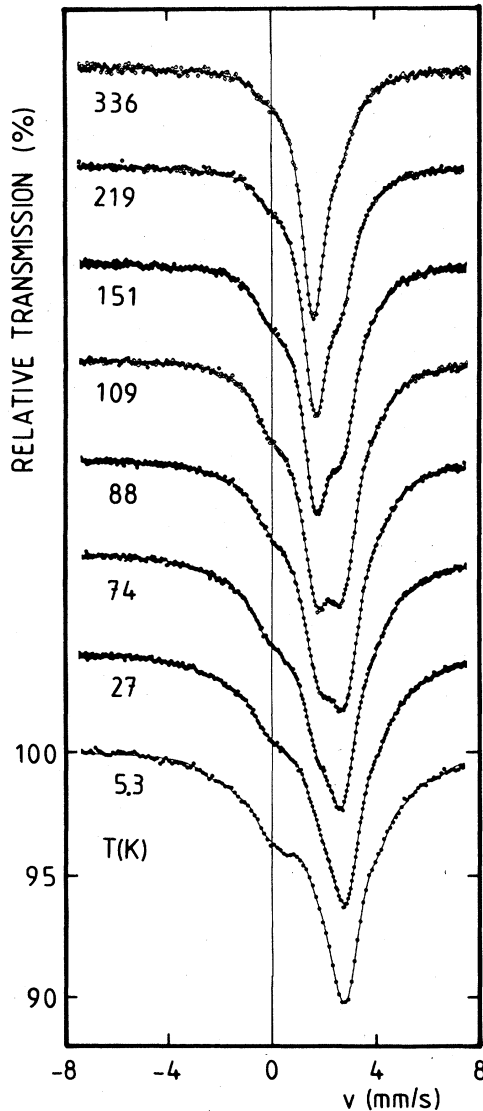


FIG. 6. ^{119}Sn -site Mössbauer spectra of the Cr-13.5 at. % Fe alloy for different T . The solid lines represent the fit using the superposition method (see text).

TABLE II. Best-fit values of the ^{119}Sn -site hf parameters as obtained with the superposition method for the 5.3-K spectrum. The meaning of the symbols is the same as those in Table I.

N	H	ΔH	I	P
0	-4.0		2.53	0.27
1	+9.6	13.6	2.20	0.21
2	+19.7	10.1	1.77	0.14
3	+32.4	12.7	1.88	0.22
4	+46.9	14.5	1.79	0.07
5	+62.1	15.2	1.80	0.09

\bar{H}_{Fe} . First of all, as deduced from the in-field Mössbauer-effect measurements (see Fig. 7) the Sn-site hf field H_{Sn} is positive. This result itself is interesting in view of the fact that H_{Sn} is negative both in a pure iron as well as in a pure chromium matrix. Therefore, the positive sign deduced for the Cr-13.5 at. % Fe alloy as well as for the Cr-25 at. % Fe alloy does not seem to be related either with the ferromagnetic or the antiferromagnetic state.

The temperature dependence of \bar{H}_{Sn} shows two anomalies: the first one at $T_I \approx 85$ K, which is close to the Néel temperature, $T_N = 90$ K of the sample⁵ and a second one at $T_{II} \approx 20$ K which is again in accord with the spin-freezing temperature as deduced above from the temperature dependences of $d\bar{H}/dT$ [Fig. 3, inset (b)] and A_M (Fig. 4). We further note that $\bar{H}_{\text{Sn}}(T)$, in the region $20 \text{ K} < T < 85 \text{ K}$, looks like a Brillouin function. For $T > 85 \text{ K}$, however, \bar{H}_{Sn} does not vanish but smoothly decreases with increasing T from ~ 15 kOe at $T \approx 85 \text{ K}$ to

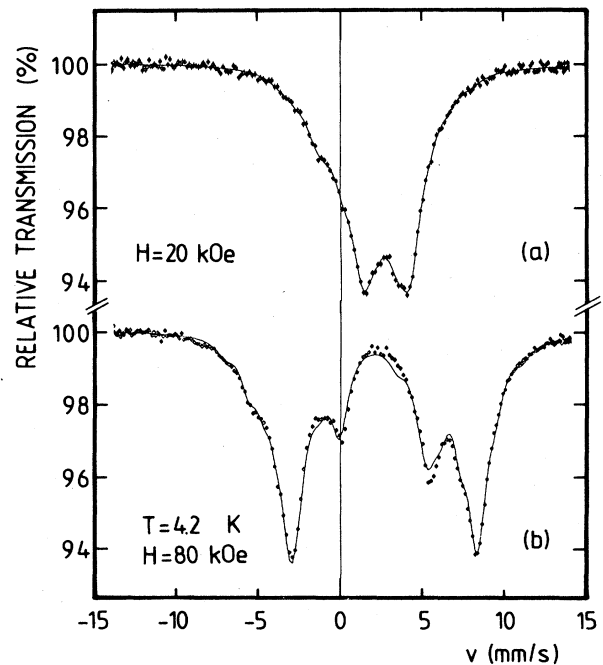


FIG. 7. ^{119}Sn -site Mössbauer spectra of the Cr-13 at. % Fe alloy taken at $T=4.2$ K in external magnetic fields of 20 kOe (a) and 80 kOe (b). The solid lines correspond to the best fit using the superposition method (see text).

~ 9 kOe at $T \approx 330$ K.

Because the Sn atoms do not develop magnetic moments of their own, H_{Sn} must be of a transferred origin, i.e., it mainly probes the spin-polarization of the lattice as a whole. The above result means that even at $T \approx 3.7T_N$ the lattice remains polarized. We have not observed such an effect with the ^{57}Fe -site measurements. This may be due to a cancellation of the negative contribution to H of the Fe core polarization with the positive contribution from the lattice.

For comparison we give in Fig. 3 the results for \bar{H}_{Sn} of the previously investigated Cr-25 at. % Fe sample (dashed line), also. As can be easily seen the behavior of both fields is very similar, except that \bar{H}_{Sn} (25 at. % Fe) is smaller for $T > T_f$. Apparently, by increasing the number of iron neighbors the lattice polarization in the ferro- and antiferromagnetic regimes is reduced, while it is increased in the spin-glass regime [\bar{H}_{Sn} (13.5 at. % Fe) $<$ \bar{H}_{Sn} (25 at. % Fe)].

As seen from Fig. 3 the spin-freezing temperature is less well defined for the Fe-rich sample (the corresponding anomaly is not so sharp). This probably, at least in part, explains the difficulties some authors faced when investigating $\text{Cr}_{1-x}\text{Fe}_x$ samples with x close to the critical concentration ($0.19 < x < 0.25$). These difficulties led them to call the alloys in this composition range as having "complex"¹ or "anomalous"¹⁰ magnetic properties. Our recent in-field Mössbauer-effect measurements³ have shown, however, that these alloys show a reentrant behavior to a spin-glass state.

In Fig. 8 we illustrate how the ^{119}Sn -site hf field for a particular atomic configuration $H^{\text{Sn}}(N)$ depends on T . There are several characteristic features worth noting. (i)

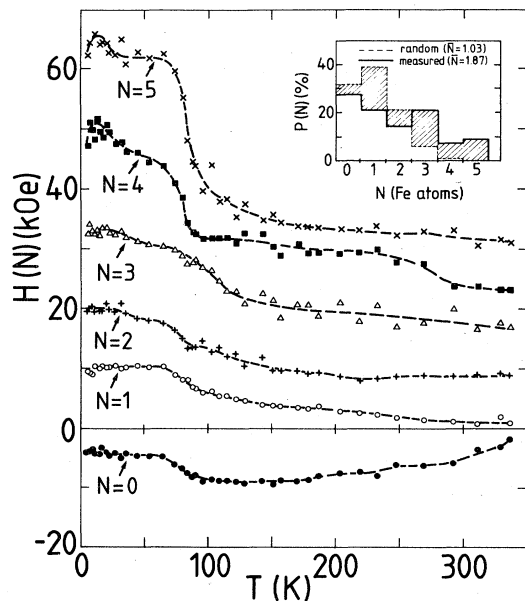


FIG. 8. ^{119}Sn -site hf fields of configurations with $N=0-5$ Fe atoms in the NN shell as a function of temperature T . The inset shows the probabilities of these configurations, $P(N)$, as measured (—) and as expected (---) for a random Fe-Cr distribution.

$H^{\text{Sn}}(0)$ is negative, in agreement with its sign in a pure chromium matrix.¹¹ However, its absolute value has been reduced by a factor of ~ 10 , which may be due to changes in the lattice polarization caused by the Fe atoms. (ii) $H^{\text{Sn}}(N)$ with $N \geq 1$ is positive and increases by 10–15 kOe per one Fe atom added. (iii) The Fe atoms exert a stabilizing influence on the antiferromagnetic state. This can be deduced from the $H^{\text{Sn}}(N)$ -versus- T curves which change from a rather flat shape for $N \leq 3$ to a Brillouin-function-like shape for $N \geq 4$. (iv) All $H^{\text{Sn}}(N)$ -versus- T curves show an anomaly at $T \approx 90$ K, being rather smeared out for $N \leq 3$ and well pronounced for $N \geq 4$ (this anomaly should reflect the Néel temperature of the alloy). (v) $H^{\text{Sn}}(N)$ -versus- T curves with $N \geq 4$ exhibit an additional anomaly at $T \approx 20$ K, which is obviously related to the spin-freezing temperature T_f . In contrast, the curves for $N \leq 3$ do not show such an anomaly. This may be taken as an evidence that T_f is closely related to a given magnetic environment, i.e., it may not be characteristic of the alloy as a whole. Such an explanation remains in agreement with our measurements on the Cr-25 at. % Fe alloy,² as well as with the results of Burke and Rainford⁵ who showed that the bulk T_f decreases with decreasing x . On a microscale each atomic configuration corresponds to a locally different x . Hence, the configurations with low N should have lower values of T_f as those with larger N .

The data for $H^{\text{Sn}}(N)$ demonstrate that the contributions of the Fe neighbors to the Sn-site hf field are additive with an average value of $\Delta \bar{H}^{\text{Sn}} = 13.2 \pm 2.0$ kOe. In the Fe-site region of the phase diagram the corresponding value was $\Delta \bar{H}_1^{\text{Sn}} = 29.8$ kOe (after Ref. 12). From these two figures it follows that the field contribution of one Fe neighbor atom is changed by $\sim 57\%$ by reducing the Fe concentration in a Cr matrix from ~ 99 to ~ 13 at. %. As we mentioned in Sec. IIIA the corresponding decrease of the magnetic moment μ amounts only to $\sim 18\%$. This emphatically shows that the existence of a simple relationship between H and μ is not justified experimentally in this system.

IV. FINAL REMARKS AND CONCLUSIONS

Application of the ME technique to our Cr-13.5 at. % Fe alloy has proved to be a useful tool for the study of its magnetic properties. It has confirmed and supported several characteristic features already known from other experiments, and it also revealed some novel aspects. In particular, we have shown, in agreement with the recently proposed phase diagram of the system,¹ that the alloy undergoes a double or reentrant phase transition on lowering T : from a paramagnetic (PM) to an antiferromagnetic (AFM) and finally to a spin-glass (SG) state. However, our present results clearly show that both transitions are not clear cut on a microscale, i.e., the system can be described neither by a single Néel temperature T_N nor by one value of the spin-freezing temperature T_f .

Concerning the latter point, we can distinguish at least two such temperatures, T_f^{NM} and T_f^{M} . T_f^{NM} is associated with the nonmagnetic phase, which in turn can be related to Fe nuclei having an average of 1.4 Fe neighbors, and

T_f^M can be attributed to the magnetic phase with an average number of 3.6 Fe neighbors. As $T_f^M > T_f^{NM}$, and because the Fe concentration in the M phase is larger than that in the NM phase, we conclude that additional Fe neighbors favor the SG phase. This is in agreement with the observations of Burke and Rainford,⁵ that up to $x \approx 0.19$, T_f increases with x . On the other hand, we observed an opposite behavior for the Cr-25 at. % Fe sample³ where the magnetic state is in general ferromagnetic. There, the freezing temperature was lowered with an increasing number of Fe neighbors. Obviously, in that case the Fe atoms stabilize the magnetic phase and depress the SG phase. Consequently, one expects that the borderline for the SG phase for $x > 0.19$ should go down to lower temperatures with increasing x . This seems to be the main difference between the $\text{Cr}_{1-x}\text{Fe}_x$ alloys for $x = 0.135$ and 0.25 .

Two interesting features which we could derive from the ^{119}Sn -site ME measurements are: (i) a change of the sign of the hf field from negative for $N = 0$ to positive for $N \geq 1$ (this occurs both for $x = 0.135$ and 0.25) and (ii) the existence of a nonzero spin polarization in the lattice well above T_N (up to $T = 3.7T_N$). The magnitude of the corresponding hf field depends on the Fe concentration x being larger for smaller x (it changes at the rate of ~ 0.25 kOe/at. % Fe between $x = 0.135$ and 0.25). It is most

likely related to the SDW which are well known to exist in a pure chromium. The addition of iron suppresses the SDW by reducing their amplitude.¹⁰ This we observe here via the ^{119}Sn -site hf field being smaller for a more concentrated sample.

On a microscale, however, the polarization is proportional to the number N of Fe atoms in the vicinity of a probe ^{119}Sn nucleus. This field increase is probably related to a different mechanism responsible for an additional contribution to the ^{119}Sn -site hf field coming from Fe atoms that are close to the probing ^{119}Sn nuclei. This may be a direct transferred hf interaction which is rather localized in its nature, contrary to the itinerant character of the SDW, and is reasonable in the light of the low relaxation rate in this system.¹³

It would be of interest to see whether the lattice is polarized for $0.16 \leq x \leq 0.19$, i.e., for the region where according to the recent phase diagram¹ a direct transition from a PM to a SG phase takes place, and if so, whether there any anomalies appear when entering the AFM and FM phases upon changing x at constant temperatures.

ACKNOWLEDGMENT

One of us (S.M.D.) thanks the Alexander von Humboldt Foundation for financial support.

*On leave from the Department of Solid State Physics, Academy of Mining and Metallurgy, PL-30-059 Krakow, Poland. Present address: Laboratoire de Métallurgie, Ecole des Mines, Parc Saurupt, F-54042 Nancy Cedex, France.

¹S. K. Burke, R. Cywinski, J. R. Davis, and B. D. Rainford, *J. Phys. F* **13**, 451 (1983).

²S. M. Dubiel, Ch. Sauer, and W. Zinn, *Phys. Rev. B* **30**, 6285 (1984).

³S. M. Dubiel, Ch. Sauer, and W. Zinn, *Phys. Rev. B* **31**, 1643 (1985).

⁴B. Window, *J. Phys. E* **4**, 401 (1971).

⁵S. K. Burke and B. D. Rainford, *J. Phys. F* **13**, 441 (1983).

⁶J. Hesse and U. Schossow, *Int. J. Magn.* **5**, 187 (1973); J. Hesse

and A. Rübartsch, *Physica (Utrecht)* **80B**, 33 (1975).

⁷H. Kuwano and Y. Morooka, *J. Jpn. Inst. Met.* **44**, 1134 (1980).

⁸S. M. Dubiel and J. Zukrowski, *J. Magn. Magn. Mater.* **23**, 214 (1981).

⁹F. Kajzar, G. Parette, and B. Babic, *J. Phys. Chem. Solids* **42**, 501 (1981).

¹⁰S. M. Shapiro, C. R. Fincher, A. C. Palumbo, and R. D. Parks, *Phys. Rev. B* **24**, 6661 (1981).

¹¹R. Street, B. C. Munday, B. Window, and I. R. Williams, *J. Appl. Phys.* **39**, 1050 (1968).

¹²S. M. Dubiel, *Hyperfine Interact.* **8**, 291 (1980).

¹³V. A. Makarov, I. M. Puzey, A. N. Koropiy, and T. V. Sakharova, *Phys. Met. Metallogr. (USSR)* **54**, 66 (1982).